

Numerical Investigation on Flow Boiling Heat Transfer in Elliptic Microchannel Heat Exchanger with Micro Fins

Bingcheng Li^a, Junming Hou^a, Weihao Ling^a, Keke Xu^b, Qiang Gao^b, Min Zeng^{a,*}

^aKey Laboratory of Thermo-Fluid Science and Engineering, Ministry of Education, Xi'an Jiaotong University, Xi'an, Shaanxi 710049, China

^bSanhua (Hangzhou) Micro Channel Heat Exchanger Co., Ltd, #2891 2th Street, Hangzhou Economic Development Area Zhejiang, 310018, China
 zengmin@mail.xjtu.edu.cn

The results of numerical research on boiling heat transfer of R410A refrigerant in an elliptic tube with four microchannels and micro fins are presented in this paper. The boiling performance of elliptic microchannel tubes with different inlet vapor qualities is studied, keeping saturation temperature constant at 278.15 K corresponding to the saturation pressure at 93,623 Pa with 3 kW/m² heat flux and 150 kg/(m²s) mass flux. The Martinelli parameter, heat transfer coefficient, pressure drop, and so on are investigated in the present paper. The CFD results are compared with and verified by the previous two-phase heat transfer correlations. The discrepancies in flow rate, heat transfer performance, and two-phase flow pattern between the middle and the two sides of the elliptic tube are compared. The velocity field and flow trajectory of gas-liquid two-phase flow in the elliptic tube microchannels are discussed and analysed. The results show that when the inlet vapor quality is high, there will be a distinct heat transfer deterioration area in the microchannels during the boiling process. The large area of gas film can weaken the heat transfer performance of the microchannel heat exchanger up to 35.42 % in the region without micro fin. The local highest heat transfer coefficient can reach 2,886.8 W/(m²K) in the physical model. The micro fins can not only increase the heat transfer area and enhance the nucleate boiling but also divide the gas film to form a local annular flow pattern and inhibit the deterioration of boiling heat transfer. The present paper is of great significance for scientific utilization and optimization of the heat exchanger, the reduction of energy consumption, and the enhancement of the exergy efficiency of the system.

1. Introduction

Enhancing the heat transfer ability of flow and boiling in microchannel heat exchangers (MCHE) remains a challenge in the design and setting of appropriate flow conditions. Li et al. (2019) conducted a numerical simulation study on evaporation temperature and dip angle of different MCHEs, but did not systematically analyse heat transfer capacity in combination with a two-phase flow pattern. Lee et al. (2022) studied the influence of different two-phase flow patterns on heat transfer performance, but the physical model was relatively simple. Silva et al. (2017) revealed that the evaporation process can be boosted by increasing the temperature when studying the alcohol. Hong et al. (2020) explored the heat transfer characteristics of radially extended MCHE through flow boiling of deionized water, but they did not study refrigerants with better phase transition capability. The process of boiling heat transfer in MCHE is more complex than that of single-phase heat transfer in traditional hydraulic diameter channel heat exchangers. There are few pieces of research on the application of micro fins in MCHE. With the continuous improvement of market and engineering requirements on heat transfer performance and size of heat exchangers, micro fins arrangement for MCHE is a significant method to optimize the boiling performance. In the present paper, a design for four channels elliptic tube with micro fins is proposed, and the flow boiling heat transfer performance is studied by numerical simulation of fluid-structure coupling strategy. The calculation results of the heat transfer coefficient are compared with the empirical correlations. The microchannel heat exchanger design with micro fins proposed in this paper can enhance the thermal performance of the flow system without huge pressure drop, which can be used as an efficient and energy-saving heat and mass transfer heat exchanger design for engineering promotion.

2. Methodology and models

2.1 Numerical method

VOF (Volume of fluid) method is a broadly used multiphase flow CFD method based on the Euler grid. The continuity equation and the local continuity equation in a phase change process are shown in Eq(1) and Eq(2).

$$\frac{\partial}{\partial t} \rho + \nabla(\rho \vec{u}) = 0 \quad (1)$$

$$\frac{\partial}{\partial t} \rho_\varphi + \nabla(\rho_\varphi \vec{u}) = +m_{vr} \text{ or } -m_{vr} \quad (2)$$

where t is the time, ρ is the density, \vec{u} is the velocity field, and φ denotes the liquid phase ($-m_{vr}$) or vapor phase ($+m_{vr}$). m_{vr} represents the mass flux rate of phase change, which can be calculated by the Tanasawa equation (Tanasawa, 1991) as Eq(3).

$$m_{vr} = \frac{C_{ta}}{2 - C_{ta}} \sqrt{\frac{2M \rho_g h_{ig} (T - T_{sat})}{R T_{sat}^{\frac{3}{2}}}} \quad (3)$$

where C_{ta} is Tanasawa coefficient, M is molecular weight, R is the vapor constant and h_{ig} represents the latent heat. The approach is a surface-tracking methodology in which fluid components that are mutually incompatible share a set of momentum equations. The volume fraction of each phase is equal to unity, according to the hypothesis. Calculating the phase fraction of each grid cell in the entire computational domain can be used to build the interface. In the present study, R410A refrigerant vapor is defined as the primary phase. The temperature and velocity are shared among the phases and the momentum equation and energy equation of the VOF model are as follows.

$$\nabla(\rho \vec{u} \vec{u}) = \nabla[\mu(\nabla \vec{u} + \nabla \vec{u}^T)] + \rho \vec{g} + \vec{F} - \nabla p \quad (4)$$

$$\nabla(\vec{u}(\rho c_p T + p)) = \nabla(\lambda \nabla T) + h_{ig} m_{vr} \quad (5)$$

where μ is the fluid viscosity, p is the pressure, λ is the thermal conductivity and \vec{F} is the external force, which can be solved by the continuum surface force model (Brackbill, 1991) as Eq(6) and Eq(7).

$$\kappa_g = -\kappa_l = \nabla \frac{\nabla \alpha_g}{|\nabla \alpha_g|} \quad (6)$$

$$\vec{F} = \frac{2\rho\sigma\kappa\nabla\alpha_l}{\rho_g + \rho_l} \quad (7)$$

where σ is the surface tension coefficient, κ is the interface curvature, and α denotes the phase fraction. The thermodynamic and transport properties ψ of the fluid are calculated by Eq(8).

$$\psi = \alpha_l \psi_l + (1 - \alpha_l) \psi_g \quad (8)$$

The temperature at the phase interface is nearly identical during the boiling phase transition process and the Clausius Clapeyron equation is adopted as a function of the temperature and pressure as Eq(9). m and n are any two points in the phase transition region. ANSYS Fluent 19.0 software is used for numerical calculation.

$$\ln \frac{P_{sat,m}}{P_{sat,n}} = \frac{M h_{ig}}{R} \left(\frac{1}{T_{sat,n}} - \frac{1}{T_{sat,m}} \right) \quad (9)$$

2.2 Physical model and boundary conditions

The computational domain in the present study is a three-dimensional model of four channels elliptic tube with micro fins. The geometric sketch, the meshes of the fluid domain, and the solid domain are shown in Figure 1. The annotation and size of the 3D model are shown in Table 1. The y^+ number is a key metric for assessing the quality of the first-layer grid, and it's an important component to consider while solving turbulence problems. The number of the fluid domain boundary layer is 8, and the height of the first layer boundary layer is 1.5×10^{-6} m, keeping the y^+ number close to 1. The R410A refrigerant with the subcooling degree of 0.01 K is used as the medium in the mesh independence validation process. The global Courant number is 0.25, and the initial time step is 10^{-6} s. A time-step adaptive scheme is used to solve transient computing problems.

Table 1: The length of symbols for 3D models

Symbols	D	Dh	R ₁	R ₂	H	H _m	H _s	L	δ	δ_{fd}	δ_{fh}
(mm)	3.630	1.700	2.540	0.250	4.050	1.530	0.820	80.00	0.520	0.100	0.300

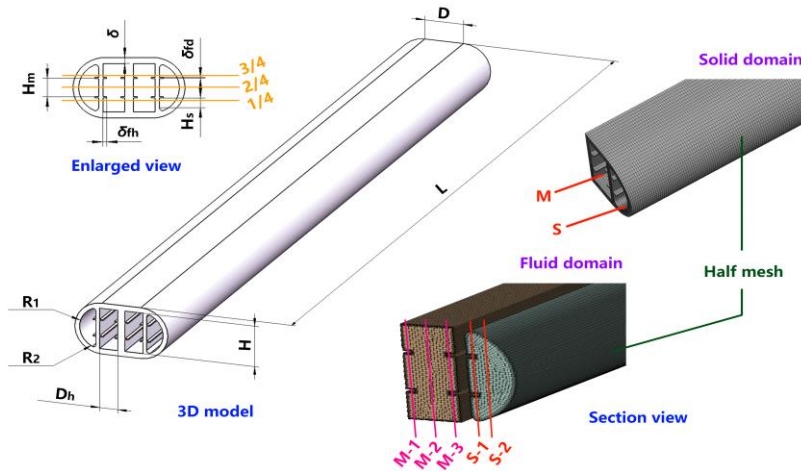


Figure 1: 3D model annotation and schematic and computational domain grids

The explicit VOF and implicit body force formulation are selected, and the double-precision solver is activated. The SST $k-\omega$ turbulence model (Menter, 1993) is used to avoid the problem that the model is too sensitive to the boundary conditions of turbulent free flow and the turbulent characteristics of inlet free flow. The fluid-structure coupling strategy is used to make the calculation conditions more similar to the real engineering practice with the consideration of the surface tension and gravity acceleration. The R410A refrigerant with a mass flow flux of $150 \text{ kg}/(\text{m}^2\text{s})$ flows into the microchannels at saturated pressure for boiling heat transfer, and the phase transition temperature is 278.16 K. Using velocity inlet and pressure outlet boundary conditions, the solid wall surface is heated by a uniform heat flux of $3 \text{ kW}/\text{m}^2$. The PISO scheme and the Geo-Reconstruct format are adopted and the adjacent correction is considered in the process of iteration.

3. Results and discussions

3.1 Methods validation

The pressure loss (ΔP) was taken as the measurement index, τ denotes the flow time and the results are shown in Figure 2a. In consideration of accuracy and efficiency, the mesh consisting of 3.32 M grid cells was selected as the calculation mesh, since the influence of increasing the number of mesh elements on the calculation result was negligible. To verify the reliability of the numerical simulation results, the classical empirical equations for gas-liquid two-phase heat transfer inside tubes were selected for comparison, as shown in Figure 2b. The numerical simulation results of the boiling heat transfer coefficient on the refrigerant side in the present paper are close to the Gungor and Winterton results (Gungor and Winterton, 1986). The variation trend is the same as that of Butterworth and Chein (Chein, 2015). And the empirical correlations predicted by Shah (Shah, 1982) and Liu and Winterton (Liu and Winterton, 1991) were also considered. The empirical correlation is usually related only to the vapor quality and physical properties of the two-phase flow. It is reasonable that there are some discrepancies in the boiling heat transfer coefficient since the pipe size and structure are diverse. In a logical range, it can be judged that the numerical simulation method proposed in this paper is convincing.

3.2 Flow heat transfer field

The vapor quality x is the ratio of the steam mass to the total mass, which is a key parameter in the study of two-phase flow heat transfer. The tube wall is heated and fluid starts boiling as τ is 0. The flow and heat transfer are inseparable, and the distribution law of the velocity field often affects the distribution of the temperature field. When the vapor quality of the refrigerant at the inlet is 0.05 and the flow heat transfer reaches a stable state, the velocity inside the microchannel oval tube, the trajectory of the fluid particle, and the heat transfer coefficient between the fluid domain and the solid domain are shown in Figure 3. The refrigerant flow path lines at the entrance of the microchannels are wavy, with large disturbances and thin boundary layers. The phenomenon is known as the entrance effect where the heat transfer is intense and the heat transfer coefficient is large.

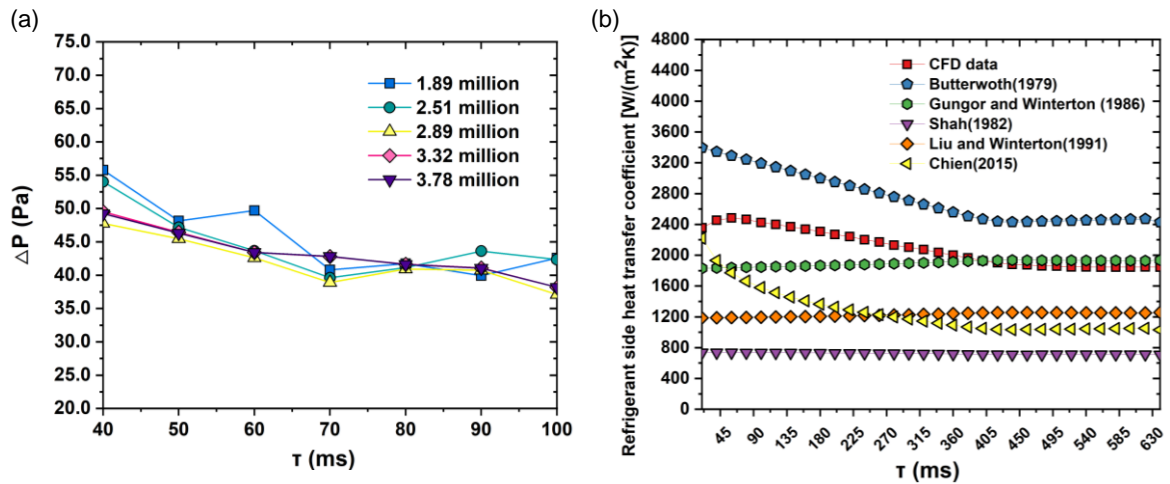


Figure 2: Methods validation: (a) Mesh independence validation, (b) Results validation

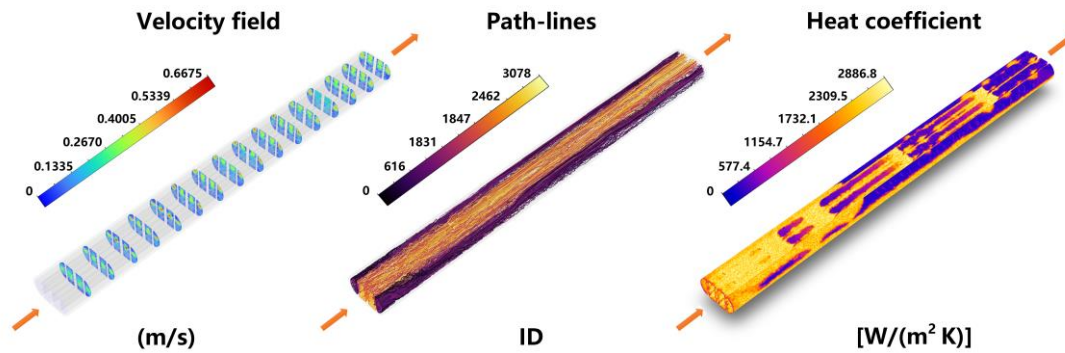


Figure 3: Flow heat transfer field contours including velocity, path lines, and heat coefficient

The normal cross-sections along the flow direction in the microchannels were established for intuitive display and discussion. The flow characteristics are close to that of single-phase flow at the initial stage of the boiling heat transfer process. The flow speed in the center of the entrance is faster and the velocity near the wall gradually diminishes. The fluid near the wall flows slowly under the action of drag force, forming a velocity gradient during the flow process. When the liquid refrigerant is heated to saturation temperature and pressure by the tube wall, the little bubbles generated during the phase change process gradually get larger and fuse into giant bubbles, which float to the top of the microchannel heat exchanger. The bubbles in the rectangle microchannels in the middle appeared earlier than that in the semi-circular microchannels on both sides. After the boiling heat transfer process is further developed, the steam gradually fills the top of the microchannels, and the liquid at saturation temperature flows in the area of the bottom of the pipeline with distinct velocity stratification and smooth movement trajectory of fluid particles. As a large amount of steam generated in boiling accumulates towards the top of the microchannel elliptic tube, a local heat transfer deterioration zone appears in the top region. The heat transfer coefficient sharply decreases since the single-phase heat transfer is dominant here, and the heat transfer performance is far less than the phase transformation.

In order for readers to have a visualized comprehension of the two-phase flow pattern in the microchannels, the feature planes are captured for contours display, as shown in Figure 4. The locations of these planes are indicated in Figure 1. The boiling phenomenon is apparent at the bottom of the microchannels of the elliptical tube and numerous tiny bubbles appear. The bubbles combine to form larger bubbles that break away from the wall and float to the top of the pipe with the buoyancy. A substantial portion of the gas film can be seen in the microchannels' central region, which is prone to local regional heat transfer deterioration. By using micro fins, the square microchannel in the middle and the semi-circular microchannels on both sides can effectively

separate large bubbles to form annular flow, which is conducive to improving boiling heat transfer coefficient and alleviating heat transfer deterioration.

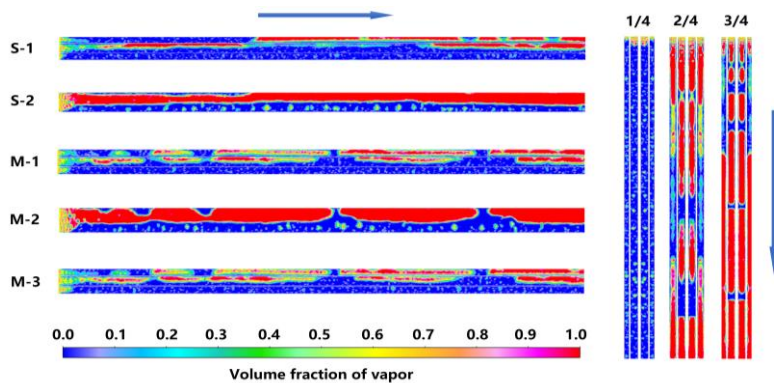


Figure 4: Flow pattern of gas-liquid two-phase flow during the boiling heat transfer process

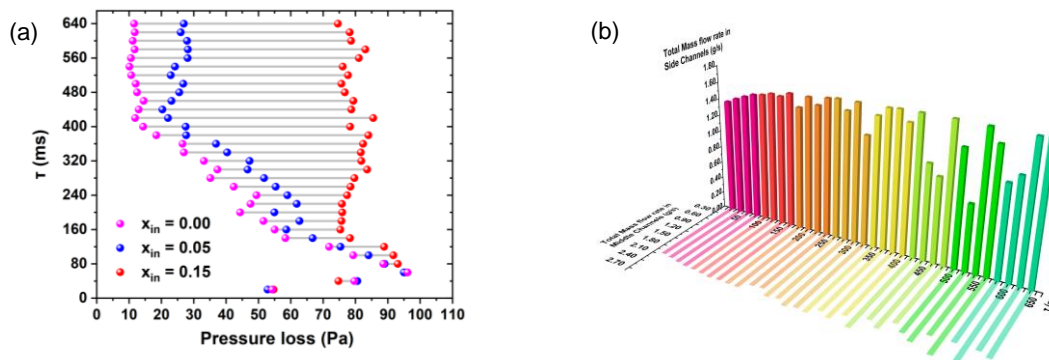


Figure 5: (a) Pressure drop between the inlet and outlet, (b) The total flow in the middle (M) and on both sides (S) of the elliptical tube microchannels

The pressure drop varies with the boiling process and the flow time (τ), as shown in Figure 5a. As the flow time reaches 440 ms, the boiling heat transfer process tends to be relatively stable, which can be regarded as dynamic thermal equilibrium. When vapor quality at the inlet is low, the pressure loss in the channels increases with the rise of the vapor quality. At the beginning of the flow, the liquid phase occupies the main part. The viscosity of the liquid phase is greater than that of the gas phase, and the drag coefficient of the liquid is bigger, contributing to the large pressure drop. When the gas-liquid two phases coexist in the microchannels, the pressure loss gradually decreases. The outlet of the elliptical microchannels with micro fins is defined as the monitoring surface for exploring the flow change with time, as illustrated in Figure 5b. The middle microchannels have a higher mass flow rate than the semi-circular microchannels on both sides. The fluctuation frequency and amplitude of mass flow between the middle channels and the two side channels differ. These variances come from the difference in the flow field and temperature field of the internal gas-liquid two-phase flow. The variation indicates that boiling heat transfer capacity is influenced by channel cross-sections with varied hydraulic diameters and shapes.

3.3 Heat transfer analysis

The Martinelli parameter (X_{tt}) is of great significance in gas-liquid flow and is a key factor in the empirical correlations of two-phase heat transfer. The formulas and results are shown in Figure 6a. When the inlet vapor quality x_{in} is 0, the value of X_{tt} is an order of magnitude larger than the value of the other two cases. Figure 6b reveals the variation of heat transfer coefficient on the refrigerant side with τ at three x_{in} degrees. The heat transfer coefficient of the microchannels with micro fins in the middle of the elliptical tube is higher than that of the two sides. The difference in heat transfer coefficient is not evident at the beginning of boiling and reached the peak at approximately 70 ms. As the flow boiling progresses, an increasing number of bubbles appear in the microchannels and the deterioration of local heat transfer impairs the overall heat transfer performance. In the present study, the higher the inlet vapor quality x_{in} , the lower the heat transfer coefficient.

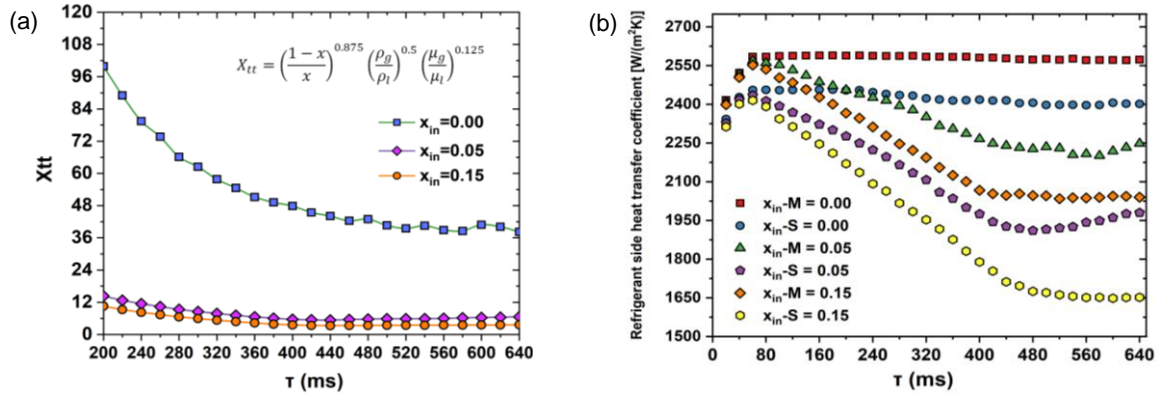


Figure 6: (a) Martinelli parameter (X_{tt}) curve with boiling time, (b) The refrigerant side heat transfer coefficient

4. Conclusions

The boiling heat transfer and pressure drop performance of four microchannels with micro fins in an elliptical tube with different inlet vapor qualities are studied by numerical simulation. The reason for the change in heat transfer performance is explained in the paper. The principal conclusions follow. The boiling heat transfer capability of the rectangular microchannels in the middle of the elliptical tube is stronger than that of the semi-circular microchannels on both sides, increasing by 4.49 %~ 19.70 % under the same working condition. The local highest heat transfer coefficient can reach 2,886.8 W/(m²K). The heat transfer deterioration occurs at the top of the MCHE where the vapor quality is high. It can not only effectively enhance the nucleate boiling and augment the heat transfer area, but also cut off the gas film to form an annular flow by installing micro fins in the elliptical microchannels. The area of heat transfer deterioration is reduced and the heat transfer capability is enhanced by the optimal design. The present study provides a convincing design for the optimization of the MCHE, which is beneficial to energy utilization rate and energy-saving.

Acknowledgments

This paper is supported by Sanhua (Hangzhou) Micro Channel Heat Exchanger Company, China.

References

- Brackbill J.U., Kothe D.B., Zemach C., 1992, A continuum method for modeling surface-tension, *Journal of Computational Physics*, 100, 335-354.
- Chien N.B., Vu P.Q., Choi K, Oh J-T., 2015, A general correlation to predict the flow boiling heat transfer of R410A in macro-/mini-channels, *Science and Technology for the Built Environment*, 21:5, 526-534, DOI: 10.1080/23744731.2015.1035603.
- Gungor K.E., Winterton R.H.S., 1986, A general correlation for flow boiling in tubes and annuli, *International Journal of Heat and Mass Transfer*, 29, 351-358.
- Hong S.H., Zhang B.H., Dang C.B., Hihara E.J., 2020, Development of two-phase flow microchannel heat sink applied to solar-tracking high-concentration photovoltaic thermal hybrid system, *Energy*, 212.
- Lawrence N., Elbel S., 2018, Numerical investigation of the effect of microchannel evaporator design and operation on the improvement potential of ejector refrigeration cycles, *Energy*, 164, 21-34.
- Lee V.Y.S., Henderson G., Reip A., Karayiannis T.G., 2022, Flow boiling characteristics in plain and porous coated microchannel heat sinks, *International Journal of Heat and Mass Transfer*, 183.
- Li G.Q., Diallo T.M.O., Akhlaghi Y.G., Shittu S., Zhao X.D., Ma X.L., Wang Y.F., 2019, Simulation and experiment on thermal performance of a microchannel heat pipe under different evaporator temperatures and tilt angles, *Energy*, 179, 549-557.
- Liu Z., Winterton R.H.S., 1991, A general correlation for saturated and subcooled flow boiling in tubes and annuli, Based on a Nucleate Pool Boiling Equation, *International Journal of Heat and Mass Transfer*, 34, 2759-2766.
- Menter, F. R., 1993, Zonal two equation k- ω turbulence models for aerodynamic flows, *AIAA Paper 93-2906*.
- Shah, M.M., 1979, A general correlation for heat transfer during film condensation inside pipes, *International Journal of Heat and Mass Transfer*, 22:547-556.
- Silva J.L., Santana H.S., Sanchez G.B., Taranto O.P., 2017, Numerical simulation of excess ethanol evaporation from biodiesel in a micro heat-exchanger, *Chemical Engineering Transactions*, 57, pp. 1123 – 1128.
- Tanasawa I., 1991, Advances in condensation heat transfer, *Advances in Heat Transfer*. 21, 55-139, doi:10.1016/S0065-2717(08)70334-4.